Torsion tests on spun-cast prestressed concrete poles

Michael Kuebler and Maria Anna Polak

- This research was undertaken to provide a better understanding of the role of helical reinforcement in prestressed concrete poles and a basis for simplifying the CSA A14-07 minimum helical reinforcing requirements.
- The results provide general information on torsional behavior of hollow, circular, prestressed concrete sections under pure torsion.
- The results suggest that helical reinforcing steel in concrete poles is most important in preventing cracking of concrete during the release of prestressing strands.

Prestressed concrete poles are commonly used as street lighting and electrical transmission poles. The governing design loads are typically bending moments as a result of wind on the arms, fixtures, and the pole itself. Typical concrete lighting poles experience little load due to torsion; however, the Canadian Standards Association (CSA) standard *Concrete Poles* CSA A14-07[1] relates the transverse (helical) reinforcing to the torsional strength of the poles. Torsion failures in prestressed concrete poles are typically sudden and brittle. Therefore, the presented testing program was designed to study the effect of helical reinforcing on the torsional strength and ductility of prestressed concrete poles.

The design and structural response of concrete poles to bending moments has been studied by several researchers.[2–4] The response of concrete poles with carbon-fiber-reinforced polymer (CFRP) prestressing reinforcement at low levels of pure torsion and in combined torsion and bending has also been investigated.[5] Little research has been completed on pure torsional capacity and torsional transverse reinforcement requirements (spacing and amount of reinforcement) for concrete poles.

The transverse reinforcement typically included in prestressed concrete poles consists of 3 mm to 6 mm (0.12 in. to 0.24 in.) wire wound helically along the length of the pole. Research suggests that more tightly spaced helical steel (less than 180 mm [7 in.]) wound in two directions would increase the torsional capacity of a pole.[6] Studies of

Table 1. Code requirements for helical reinforcement spacing for the tested specimens

CCode			ASTM C 1089-06			CSA A14-07 class C*		
Location on pole			Top 0.3 m	Middle	Bottom 0.3 m	≤1.5 m from tip	1.5 m to 4.5 m from tip	≥4.5 m from tip†
Minimum transverse reinforcement ratio, %			0.1	0.1	0.1	0.35	0.20	0.15
Transverse spacing, mm	165 mm tip	45 mm wall	25	100	25	60	110	140
	210 mm tip	55 mm wall	25	100	25	50	90	120

* CSA A14-07 allows single helix at spacing given in table or double helix of steel at double the spacing.
† This region was not used in this work because the specimens' test zone was up to 3.7 m from the tip.
Note: 1 mm = 0.0394 in.; 1 m = 3.28 ft.

the response of spun-cast concrete poles to vehicle impact loads concluded that thick walls and closely spaced spirals increase the impact resistance of concrete poles.[7] Research indicates that closely spaced (80 mm to 100 mm [3 in. to 4 in.]) steel spirals (4 mm to 5 mm [$^5/_{32}$ in. to $^3/_{16}$ in.] in diameter) are needed to resist temperature stresses, transfer forces at the pole ends, and also to contribute to the torsional and shear strength of the member.[8] An investigation into static-cast prestressed concrete poles under bending moments suggested that spiral reinforcement be placed along the entire length of the pole to control longitudinal cracking in overload situations.[4]

CSA A14-07 specifies the minimum helical reinforcing ratios for different classes of concrete poles. The helical reinforcing ratios in CSA A14-07 (specified as percentages of the concrete cross section) are detailed and vary along the length for each class of pole. Each class has assigned minimum torsional capacities. By assigning classes to the poles and varying the helical reinforcement based on these classes, CSA A14-07 implies that the helical reinforcement influences the torsional capacity of a pole. In addition, CSA A14-07 allows two methods for the placement of the helical reinforcement: as a tight single helix along the length of the pole or as an overlapping double helix consisting of two single helical wires wound in opposite directions. However, the rationale behind these design recommendations and their complexity is not clear and is not addressed in any code commentary.

ASTM C 1089-06[9] and an ASCE-PCI Committee report[10] on prestressed concrete poles govern the production of poles in the United States. The ASCE-PCI report specifies a minimum area of spiral steel as 0.1% of the concrete wall area in a unit length increment. The committee report also indicates a minimum pitch for the helical reinforcement of $^4/_3$ of the maximum aggregate size (for typical 19 mm [$^3/_4$ in.] aggregate, this translates to 25 mm [1 in.]) and not less than 25 mm. The maximum pitch should not exceed 100 mm (4 in.), unless testing shows that performance is not impaired. Clearly, the pole manufacturing provisions are simpler than the CSA A14-07 requirements and suggest different values for the minimum amount of helical reinforcing.

The pitch or spacing of the helical reinforcing is calculated based on the wall thickness and the helical reinforcing percentages given in each code. Eq. (1) is a simplified design formula for the spacing of helical reinforcement ignoring tapering of the wall thickness.

$$s = \frac{A_s}{\rho_s w} \tag{1}$$

where

s = spacing of the helical reinforcing

A_s = area of one helix

ρ_s = given reinforcing percentage

w = assumed wall thickness

The derivation of Eq. (1) as given in the ASCE-PCI report. **Table 1** summarizes the differences between the suggested spacing values for the specimens tested in this program calculated according to CSA A14-07 and ASTM C 1089-06.

This research was undertaken to provide a better understanding of the role of helical reinforcement in prestressed concrete poles and to allow a rational simplification of the CSA A14-07 minimum helical reinforcing requirements. In addition to the main purpose of the evaluation and simplification of the CSA A14-07 manufacturing requirements, these results provide general information on torsional behavior of hollow, circular, prestressed concrete sections under pure torsion.

Table 2. Specimen design dimensions of CSA A14-07 Class C pole specimens		
Tip diameter, mm	165	210
Butt diameter, mm	245	290
Taper, mm/m	15	15
Length, m	5.35	5.35
Tip wall thickness, mm	45	55
End wall thickness at 5.35 m from tip, mm	55	65
Helical reinforcing targets in tip section, %	0.35 (CSA A14-07 standard) and 0.18	0.35 (CSA A14-07 standard) and 0.18
Helical reinforcing targets in butt section, %	0.20 (CSA A14-07 standard) and 0.10	0.20 (CSA A14-07 standard) and 0.10

Note: 1 mm = 0.0394 in.; 1 m = 3.28 ft.

These tests are unique; to the best of the authors' knowledge, torsional behavior of prestressed concrete poles under pure torsion has not been reported in the literature.

Test program

A total of 14 CSA A14-07 class C (Table 1) pole specimens were produced for the test program. Seven specimens (165 group, specimens P1 to P7) had tip diameters of 165 mm (6.5 in.), while the remaining seven (210 group, specimens P8 to P14) had 210 mm (8.3 in.) tip diameters. All design targets (**Table 2**) were kept constant for each specimen except for helical reinforcing spacing and direction. The experimental program notation used to identify the specimens is as follows:

- 165 = 165 group
- 210 = 210 group
- C = control, no helical reinforcement
- CW-N = single helix, clockwise direction, normal spacing according to CSA A14-07
- CCW-N = single helix, counterclockwise direction, normal spacing according to CSA A14-07
- CW-L = single helix, clockwise direction, large spacing at twice the CSA A14-07 requirements (equivalent to half the reinforcing placed in the –D specimen)
- CCW-L = single helix, counterclockwise direction, large spacing at twice the CSA A14-07 requirements (equivalent to half the reinforcing placed in the -D specimen)
- D = double helix, one helix wound in each direction to form overlapping system, each helix spaced at twice the spacing of the CSA A14-07 requirements

Table 3 lists descriptions and differences among the specimens**.** For each group, three specimens were produced according to CSA A14-07: one specimen (-D, specimens P5 and P12) had a double helix (**Fig. 1**), and the other two were reinforced using a single helix wound in opposite directions (clockwise helix, CW-N specimens P-6 and P-13 and counterclockwise helix, CCW-N specimens P-7 and P-14). The target tip and butt helical reinforcing percentages for these specimens were 0.35% and 0.20% for the tip and butt sections, respectively. To achieve the same reinforcement percentage as the single helix, the spacing of the double helical reinforcement is twice that of a single helix. The two single-helix specimens were identical except that their helical reinforcement wound in opposite directions, one clockwise and the other counterclockwise (Fig. 1). The torsional load was applied counterclockwise to all specimens to theoretically cause tension or compression in the helical steel.

The remaining four poles for each group were not produced according to CSA A14-07. Two poles contained no helical steel (specimens P-1, P-2, P-8, and P-9), while the other two poles had single helical reinforcement at a pitch of twice the CSA A14-07 standard spacing (Fig. 1): one with helical steel in the clockwise direction (P-3 and P-10) and the other in the counterclockwise direction (P-4 and P-11). The target tip and butt helical reinforcing percentages for the non–CSA A14-07 standard poles were 0.18% and 0.10%, respectively. The larger (doubled) spacing for the single-helix specimens is equal to the normal spacing of the double helix. Therefore, these specimens (P-3 [165-CW-L], P-4 [165-CCW-L], P-10 [210-CW-L], P-11 [210-CCW-L]) had half the CSA A14-07–required spiral reinforcement. The poles not meeting CSA A14-07 were produced to observe the effect of increasing the spacing of the helical steel on the torsional response of the pole, to compare the response of the single helix with double spacing with the double-helix specimens, and to compare the behavior of all specimens with the unreinforced poles. The test concrete poles were based on an 11-m-long (35 ft) CSA A14-07 class C lighting pole design. Only a 3.0 m

Table 3. Specimen description

Specimen number	Pole identification	Description	Spacing for first 1.5 m from tip, mm	Spacing for remainder of specimen, mm	Target helical reinforcing, %	
					Tip	Butt
P-1	165-C	No helical reinforcement, control	n.a.	n.a.	n.a.	n.a.
P-2	165-C-2	No helical reinforcement, control	n.a.	n.a.	n.a.	n.a.
P-3	165-CW-L	Single helix, clockwise	120	200	0.18	0.10
P-4	165-CCW-L	Single helix, counterclockwise	120	200	0.18	0.10
P-5*	165-D	Double helix, half helix	120	200	0.35	0.20
P-6*	165-CW-N	Single helix, clockwise	60	100	0.35	0.20
P-7*	165-CCW-N	Single helix, counterclockwise	60	100	0.35	0.20
P-8	210-C	No helical reinforcement, control	n.a.	n.a.	n.a.	n.a.
P-9	210-C-2	No helical reinforcement, control	n.a.	n.a.	n.a.	n.a.
P-10	210-CW-L	Single helix, clockwise	100	170	0.18	0.10
P-11	210-CCW-L	Single helix, counterclockwise	100	170	0.18	0.10
P-12*	210-D	Double helix, half helix	100	170	0.35	0.20
P-13*	210-CW-N	Single helix, clockwise	50	85	0.35	0.20
P-14*	210-CCW-N	Single helix, counterclockwise	50	85	0.35	0.20

* CSA A14-07 design
Note: n.a. = not applicable. 1 mm = 0.0394 in.

(9.8 ft) test length is required to perform torsional testing per CSA A14-07 clause 7.4.4.2. Therefore, including the clamping length, the specimens were manufactured at a length of 5.35 m (17.6 ft). Table 2 summarizes the specimen design dimensions. The taper for all poles from tip to butt was 15 mm/m (0.18 in./ft). The target 28-day concrete compressive strength was 60 MPa (8700 psi), with minimum one-day strength of 25 MPa (3600 psi). The poles were prestressed longitudinally with four 9.5 mm ($^3/_8$ in.) prestressing strands spaced evenly around the poles' cross sections at 90° **(Fig. 2)**.

Stressing was performed to 80% (1488 MPa [216,000 psi]) of the strands' ultimate stress (1860 MPa [270,000 psi]). The transverse reinforcement (spirals) consisted of 3.5-mm -diameter (0.14 in.), smooth, galvanized, cold drawn wire helixes with a minimum yield strength of 500 MPa (72,500 psi) and an ultimate tensile strength of 600 MPa (87,000 psi) per CSA A14-07. The spacing of the helical steel was the main test parameter in this work (Table 3). The 165 group poles were designed to have wall thicknesses of 45 mm (1.8 in.) and 55 mm (2.2 in.) for the tip and the butt ends (5.35 m from the tip), respectively. For the 210 group poles, the tip wall thickness was designed as 55 mm and the butt end wall thickness as 65 mm (2.6 in.). Based on the design dimensions and materials, the unfactored cracking torque values at 0.6 m (2 ft) from the tip end using CSA's *Design of Concrete Structures* CSA A23.3-04[11] cracking torque formula were 7.1 kN-m (5.2 kip-ft) and 12 kN-m (8.9 kip-ft) for the 165 mm tip and 210 mm tip poles, respectively.

Test setup

The pole specimens were tested at the manufacturer's plant. A clamp (butt clamp) fixed to a concrete slab was used to hold the butt end of the pole rigid during testing (**Fig. 3**). To ensure fixity at the butt end, the pole was marked at the clamp, which was checked throughout the test. A counterclockwise torque was applied to each specimen. The steel cable was attached to the pole using a steel collar (tightly clamped) located 0.6 m (2 ft) from the tip of the pole as required by CSA A-14-07. The loads were applied from the pulling bench using a steel cable and a manual two-speed winch (**Fig. 4**). Possible slippage and movement of the collar were monitored during testing by marking the collar and the pole. The torque arm to the center of the pole's cross section was 0.5 m (1.6 ft). To ensure only torsional loads were applied to the specimens, a tieback cable was attached to the pole using a loose-fitting steel collar and fixed in the opposite direction of the pulling bench. This tieback cable sustained the load applied

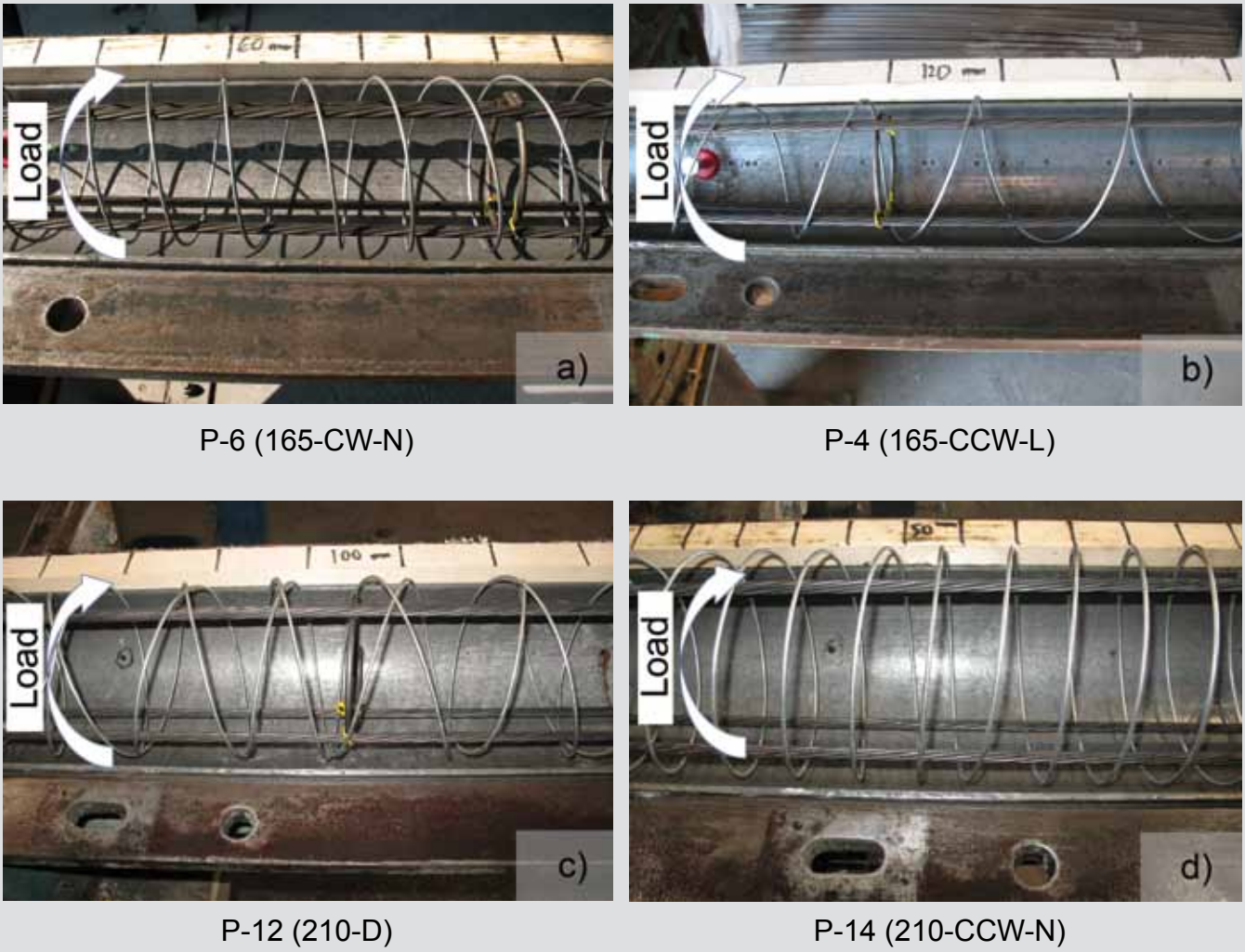

Figure 1. Example helical reinforcing layouts.

Figure 2. Cross section of a typical prestressed concrete pole showing the four prestressing-strand locations spaced at 90°.

from the pulling bench, ensuring that no bending moment in the horizontal plane was applied to the pole. During testing, some bending moment from the self-weight was introduced because the pole specimens were held in the horizontal position. Applied loads were recorded using a load cell attached between the loading collar and the loading cable. Twist values were recorded using an electronic clinometer attached at the tip end of the pole.

The tested length of specimens was 3.6 m (11.8 ft), measured from the tip to the butt clamp. A manual winch was used to apply torsion at a constant twist rate. The average twist rate was 0.7°/min. Because the loading was applied in a displacement controlled mode, testing was continued after cracking and failure to record the postpeak behavior. Testing was completed once the specimen fell to the ground, or at approximately 13° to 15° of twist at the tip of the pole when continual rotation occurred at a constant load. Measurements were also taken after testing to determine the failure location, wall thickness, and cover to the prestressing steel.

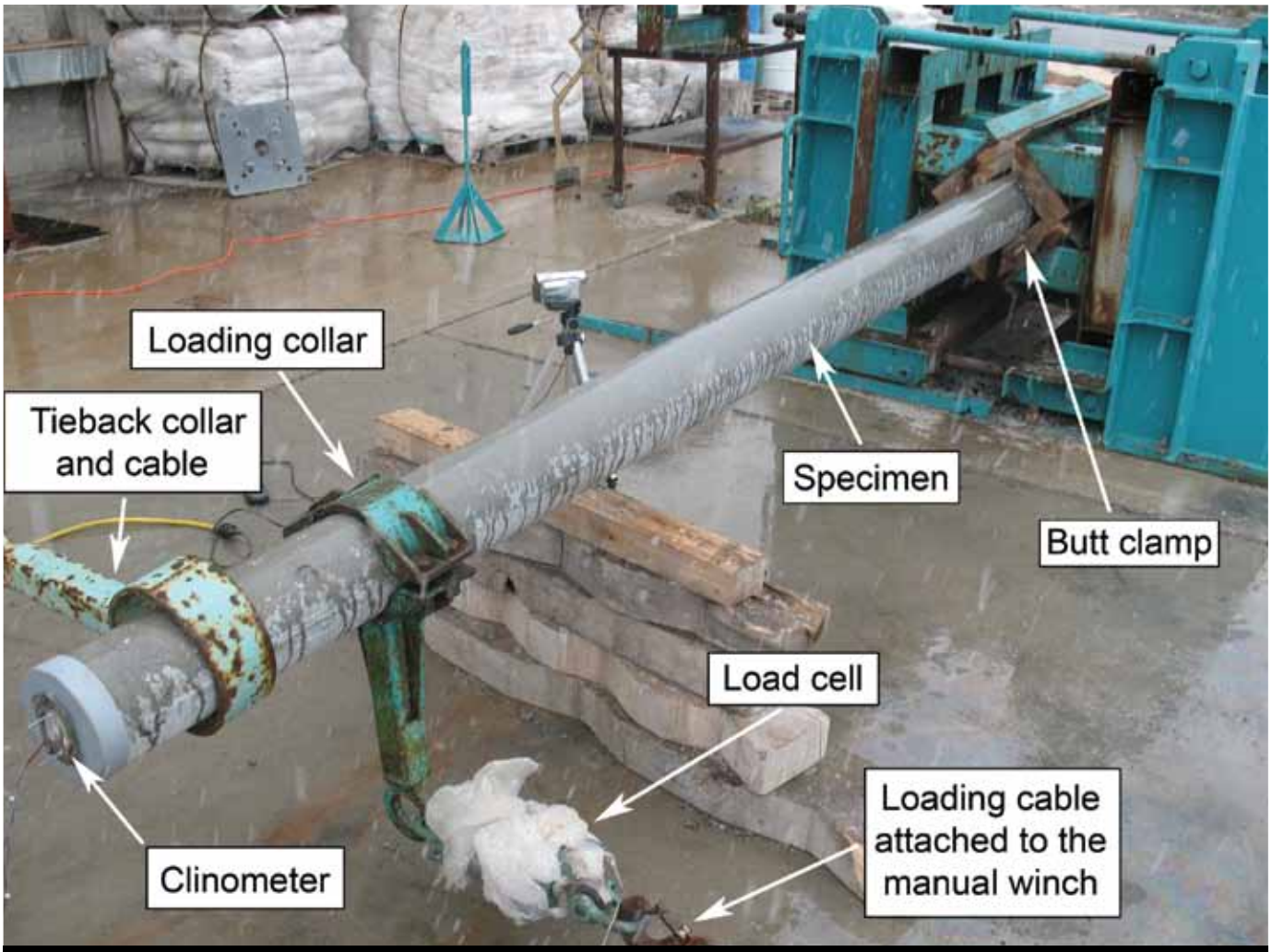

Figure 3. Loaded test setup with unreinforced 165 mm (6.50 in.) tip control specimen P-2 (165-C-2).

Test observations

Before testing, failure was anticipated to occur at the smallest loaded cross section, that is, near the loading collar. However, in this region (0.6 m [2 ft] from the end) the spacing of the helical steel was the shortest (Table 3). Figure 4 gives a summary of the terminology used to describe the testing process and observations. **Figure 5** includes full specimen test responses (including postpeak response) for all specimens. **Table 4** presents a summary of the test results and observations for the 165 group and 210 group, respectively.

For the 165 group (Table 4), five of the seven poles failed at the loading collar (**Fig. 6**) while the remaining two (P-6 [165-CW-N] and P-3 [165-CW-L]) failed at the butt clamp. Interestingly, the butt clamp failures did not have substantially higher cracking torque values than the collar failures, despite the larger diameter and volume of the concrete at the butt end. For the 210 group (Table 4) six specimens failed at the butt clamp (**Fig. 7**) and only the P-13 (210-CW-N) specimen failed at the loading collar. For the 210 group specimen, the shorter spacing of the spirals (due to the CSA A14-07 requirements, the spiral spacing for the thicker-walled 210 group was shorter than for the 165 group) could have increased the strength of the specimens near the loading collar, causing failure to occur at the butt end of the pole (the tighter spacing of spirals was for the first 1.5 m [4.9 ft] from the tip [Fig. 4]). Variations in the pole geometry or concrete mixture may also have been a factor. The 165 group had thinner walls with wider spiral spacing than the 210 group; this could have resulted in cracking of the walls near the loading collar due to prestressing transfer, which could have caused torsional failure near this collar.

In all cases, torsional cracking was initiated on the side opposite where the load was applied and moved toward the tip of the pole, spiraling to the loading side of the specimen (Fig. 4). The torque-twist plots of all specimens showed a visible cracking torque point where the curves became nonlinear (Fig. 5). In some cases, the cracking torque was the ultimate torque reached by the specimen. In other cases, additional torque was sustained momentarily after cracking, possibly due to the presence of the helical steel and the interlocking of the cracked concrete. Immediately after the cracking torque was reached, popping sounds were heard as the helical steel failed in tension.

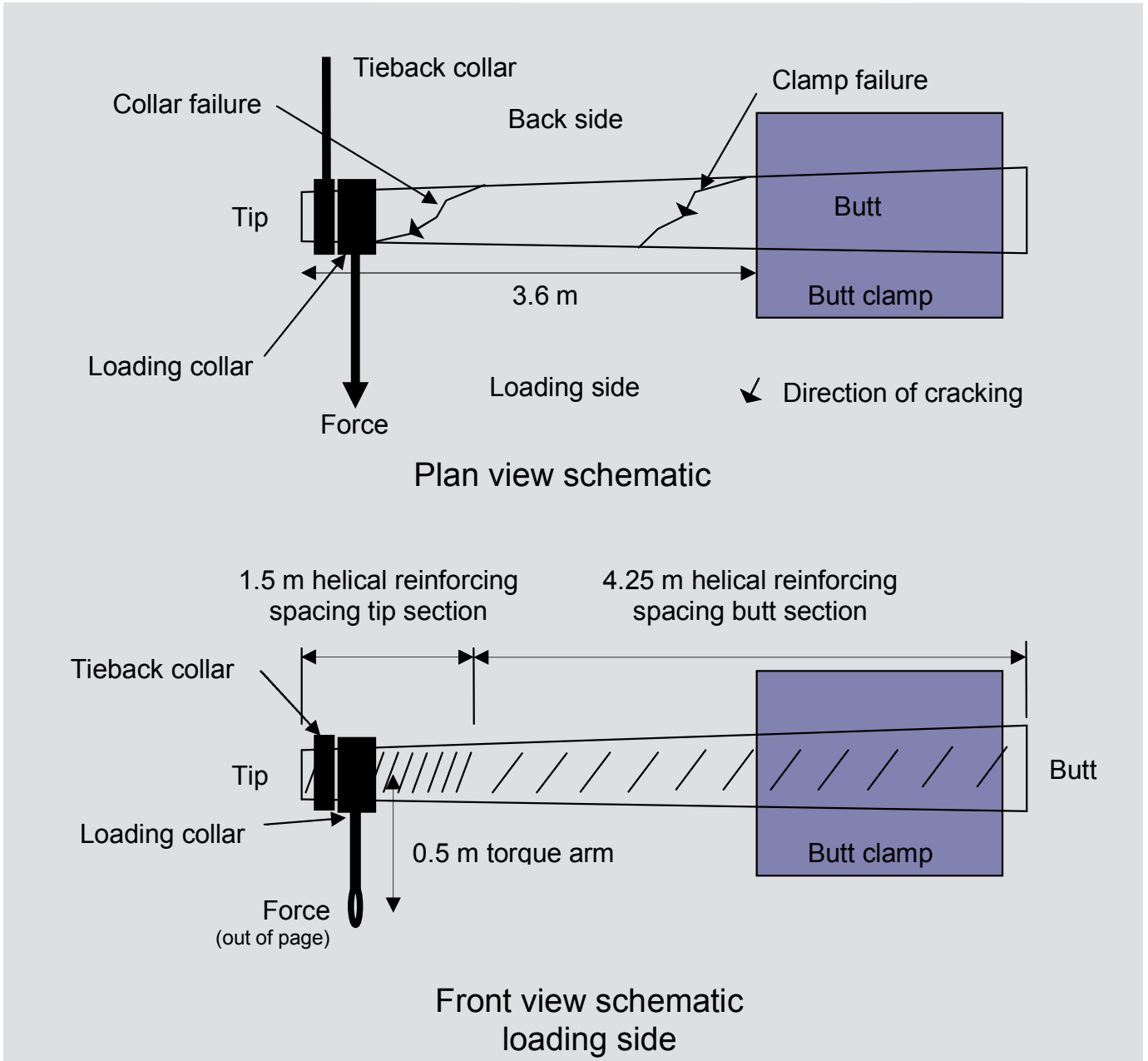

Figure 4. Schematic diagram of cracking patterns, failure locations, and loading terminology. Note: 1 m = 3.281 ft.

In all cases, the failure exhibited by the specimens was sudden and brittle with no postcracking load increase and with substantial rotation of the pole tip. The load sustained in the postcracking region was typically less than half the maximum torque (Fig. 5). The control specimens with no helical reinforcement cracked at lower torsional loads than the helically reinforced specimens.

Analysis of the test results

In prestressed concrete poles, the helical reinforcing steel area is small. Therefore, the ultimate torsional capacities calculated in accordance with CSA A23.3-04, the American Concrete Institute's (ACI's) *Building Code Requirements for Structural Concrete (ACI 318-08) and Commentary (ACI 318R-08)*,[12] and *Eurocode 2: Design of Concrete Structures, Part 1-1: General Rules and Rules for Buildings*,[13] all of which are based on space truss models and dependent on the transverse, helical reinforcing steel ratio, are lower than the cracking torque values.[14]

The experimental behavior of the specimens indicated a linear elastic response and failure caused by cracking, followed by a rapid decrease in postpeak strength and breaking of the helical reinforcement. The helical steel should therefore be ineffective before cracking because the calculation of the cracking torque depends on the concrete alone.

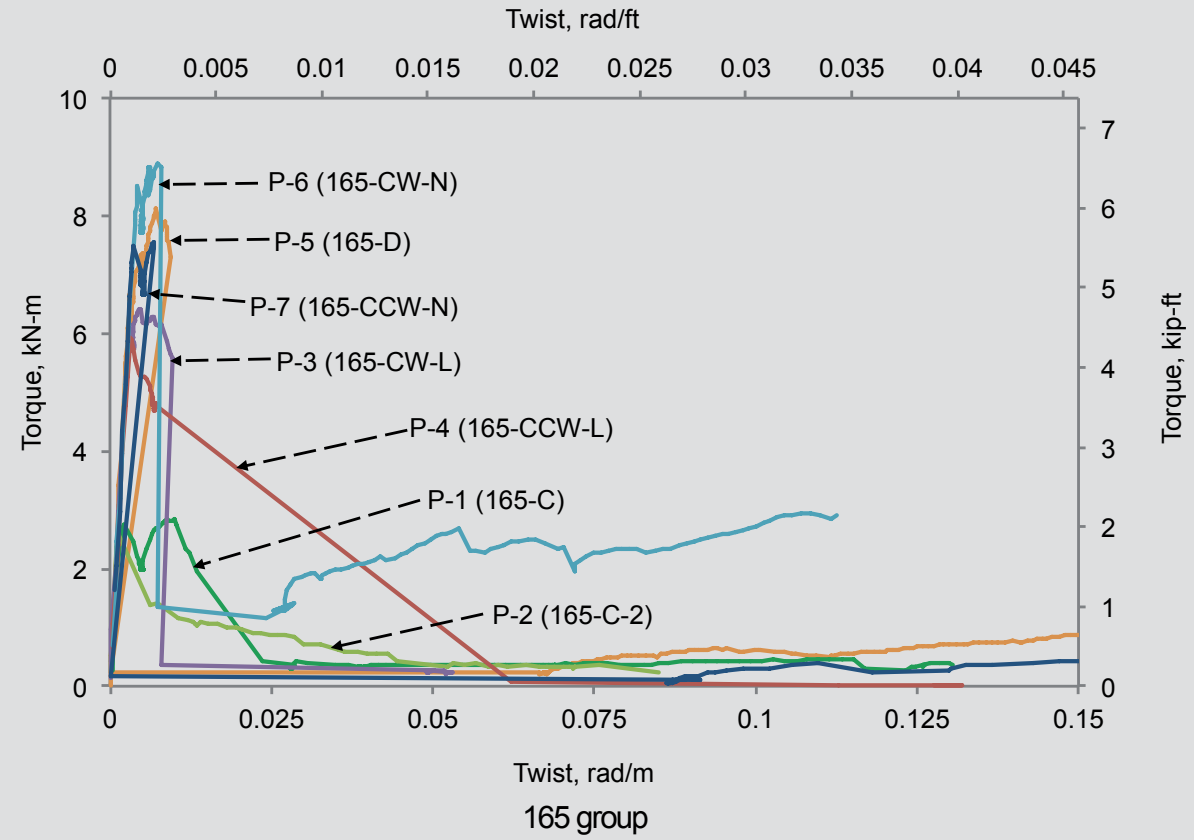

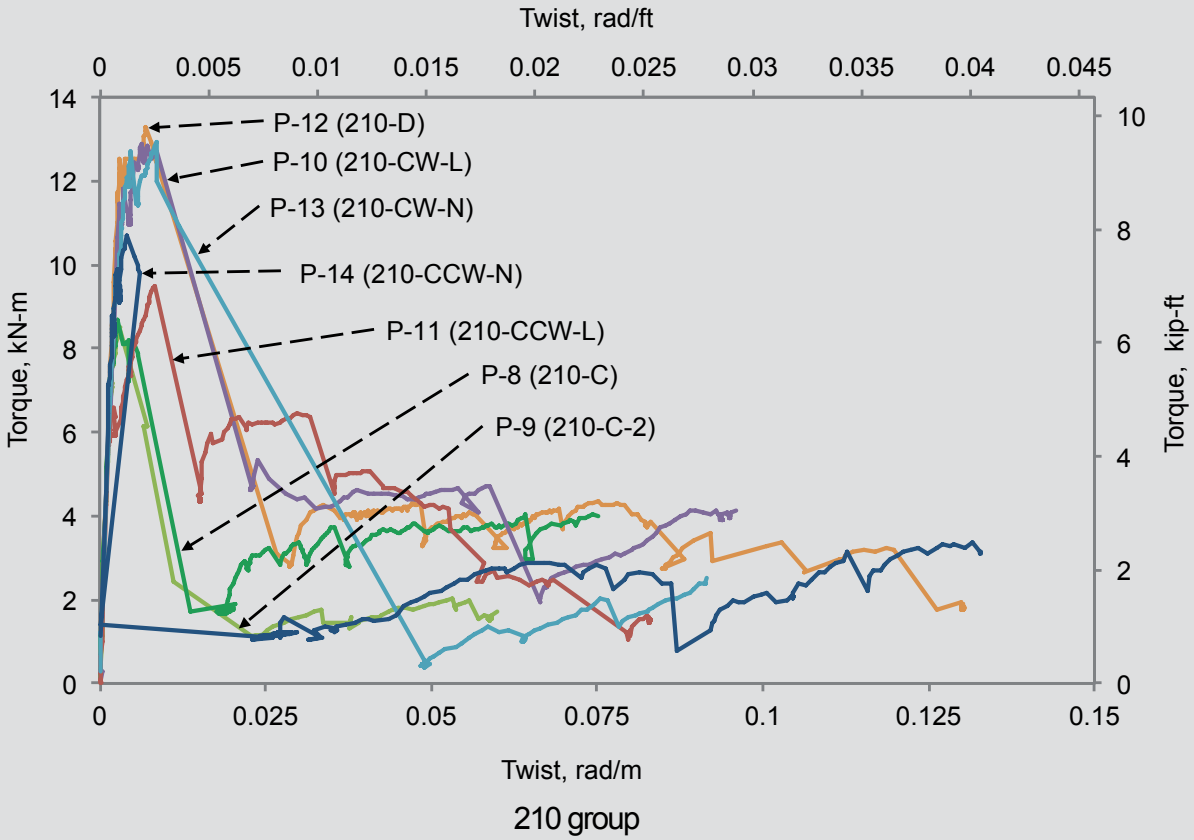

Figure 5. Full torque-twist response of test specimens.

Table 4. Summary of observation and experimental results

Specimen number	Pole identification	Specimen properties						
		Helical reinforcing spacing tip section, mm*	Helical reinforcing spacing butt section, mm*	Tip thickness, mm	Butt thickness, mm at 5.75 m	Compressive strength, MPa	Tensile strength, MPa	
P-1	165-C	n.a.	n.a.	44	64	50.6	3.5	
P-2	165-C-2	n.a.	n.a.	44	70	72.3	4.7	
P-3	165-CW-L	120	200	46	72	45.8	2.9	
P-4	165-CCW-L	120	200	46	66	64.7	4.1	
P-5	165-D	60†	100†	46	69	66.4	4.4	
P-6	165-CW-N	60	100	48	67	63.7	4.5	
P-7	165-CCW-N	60	100	45	70	66.0	4.4	
P-8	210-C	n.a.	n.a.	45	74	61.5	3.3	
P-9	210-C-2	n.a.	n.a.	50	77	68.1	3.8	
P-10	210-CW-L	100	170	53	85	57.0	4.2	
P-11	210-CCW-L	100	170	50	78	62.6	3.9	
P-12	210-D	50†	85†	52	77	65.3	4.3	
P-13	210-CW-N	50	85	50	75	67.5	4.9	
P-14	210-CCW-N	50	85	55	80	63.6	4.4	

* Tip section refers to the first 1.5 m from tip of pole; butt section refers to 1.5 m to 5.75 m from tip of pole.
† 165-D or 210-D spacing is double the value for each half helix; two halves combined values shown.
Note: n.a. = not applicable; n.d. = no data. 1 mm = 0.0394 in.; 1 m = 3.281 ft; 1 kN = 0.225 kip; 1 MPa = 145 psi.

Cracking torque

All cracking torque formulas in the codes of practice (CSA A23.3-04, ACI 318-08, and Eurocode 2) are derived from Bredt's thin-tube theory. The derivations of the code formulas are explained in a code background paper[15] that presents Bredt's thin-tube theory relating the shear stresses due to torsion τ in a thin-walled tube as Eq. (2).

$$\tau = \frac{T}{2A_o t} \quad (2)$$

where

T = applied torque

A_o = area enclosed by the shear flow path

t = thickness of the member

The shear stress is set equal to the tensile strength of concrete in biaxial tension-compression, and the effect of the prestress on the principal tensile stress is derived using Mohr's circle and is included as a factor $\sqrt{1 + \frac{f_{pc}}{f_t}}$, where f_{pc} is the stress in concrete section due to prestressing and f_t is the concrete tensile strength.[16] The biaxial stress state due to the prestressing increases the tor-

	Experimental results							
Final prestressing stress, MPa	Cracking torque, kN-m	Twist at cracking, rad/m	Stiffness, kN-m²/rad	Ultimate torque, kN-m	Twist at ultimate torque, rad/m	Failure location	Failure position from tip, m	Wall thickness at failure, mm
1116	2.8	0.0022	1281	2.8	0.0088	Collar	1.05	48
1070	2.6	0.0011	2363	n.d.	n.d.	Collar	0.80	52
1059	6.1	0.0032	1930	6.4	0.0047	Clamp	3.21	53
1052	5.9	0.0032	1876	n.d.	n.d.	Collar	0.80	49
1059	6.7	0.0032	2123	8.1	0.0071	Collar	0.90	50
1089	8.5	0.0041	2057	8.9	0.0073	Clamp	3.31	56
1059	7.5	0.0036	2055	7.5	0.0067	Collar	0.80	50
1116	5.1	0.0011	4733	8.5	0.0029	Clamp	2.20	57
1070	7.3	0.0016	4647	8.7	0.0028	Clamp	3.20	62
1059	11.5	0.0029	3894	12.9	0.0063	Clamp	3.40	68
1052	6.5	0.0016	4164	9.5	0.0084	Clamp	3.30	71
1059	12.5	0.0030	4243	13.3	0.0070	Clamp	3.30	63
1089	9.8	0.0024	4132	12.9	0.0087	Collar	0.90	55
1059	7.1	0.0013	5561	10.7	0.0041	Clamp	3.00	71

sional cracking strength. This results in a general formula (Eq. [3]) for cracking torque T_{cr}.

$$T_{cr} = f_t 2A_o t \sqrt{1 + \frac{f_{pc}}{f_t}} \quad (3)$$

ASTM C-1089-06 refers to the *Standard Specifications for Structural Supports for Highway Signs, Luminaires and Traffic Signals* (AASHTO LTS-5-M)[17] and the ASCE-PCI guide[10] for torsional design formulas. The torque formulas in these codes are identical to the ACI-318-08 cracking torque formula. Similarly, CSA A14-07 refers to CSA A23.3-04.

In ACI-318-08 and CSA A23.3-04, the thickness t is approximated as $0.75A_{cp}/p_{cp}$ and A_o is taken as $^2/_3A_{cp}$, where p_{cp} is the perimeter of the concrete and A_{cp} is the area enclosed by this perimeter. This gives Eq. (4).

$$2A_o t = A_{cp}^2 / p_{cp} \quad (4)$$

The concrete tensile strength f_t is $0.33\sqrt{f_c'}$ for ACI 318-08 and $0.38\sqrt{f_c'}$ for CSA A23.3-04, where f_c' is the concrete compressive strength in MPa.

The European pole standards EN 12843[18] and EN 40-4[19] reference Eurocode 2 to calculate the torsional capacities

Figure 6. Typical loading collar failure.

of poles. The general formula (Eq. [2]) for cracking torque is used with the parameters in Eq. (5).

$$2A_o t = 2A_k t_{ef,i} \tag{5}$$

where

A_k = area enclosed by the centerline of the shear flow including hollow area

$t_{ef,i}$ = effective wall thickness = A/u but not less than twice the distance between the edge and center of the longitudinal reinforcement (hollow sections use real thickness as an upper limit)

A = total area of the cross section including hollow areas

u = circumference of the cross section

Equation (6) defines the concrete tensile strength f_t.

$$f_t = f_{ctd} \tag{6}$$

where

f_{ctd} = design concrete tensile strength

$= 0.7 f_{ctm}$

f_{ctm} = mean axial tensile strength

$= 0.30 f_{ck}^{2/3}$ for $f_{ck} \le 50$ MPa (7300 psi) concrete

$= 2.12 \ln\left(1 + \frac{f_{cm}}{10}\right)$ for $f_{ck} > 50$ MPa (7300 psi) concrete

f_{ck} = characteristic concrete compressive strength = f_c'

f_{cm} = mean compressive strength at 28 days

$= f_{ck} + 8$

Using ACI 318-08, CSA A23.3-04, and Eurocode 2 crack-

Figure 7. Typical butt clamp failure.

ing torque formulas and parameters, averages of the ratio between the experimental and theoretical values were calculated (**Fig. 8**). A ratio below 1.0 indicated an unconservative prediction of the specimens' cracking torque. The collar location (2 ft [0.6 m] from tip) was used to calculate the torsional cracking strength because this location had the smallest cross section within the test region. The average experimental to theoretical ratio was 0.83 for ACI-318-08, 0.76 for CSA A23.3-04, and 0.65 for Eurocode 2 (**Table 5**). Using the actual failure location geometry rather than the smallest cross section lowered the ratios to 0.65, 0.6, and 0.51, respectively.

It is suspected that the control specimens (P-1 [165-C], P-2 [165-C-2], P-8 [210-C], and P-9 [210-C-2]) were cracked longitudinally before testing. Without any helical reinforcement, the poles were susceptible to cracking due to the transfer of the prestressing force (the 165 group more so than the 210 group due to thinner walls). Their lower torsional capacities are attributed to the longitudinal cracking observed along the prestressing strand. Therefore, the statistical analysis was done with and without control specimens. With the control specimens removed, the average ratios increased, as expected (Table 5). Without the control specimens, the average was more accurate and closer to a conservative value. The high and low values, however, correspond to a significant spread and indicate that either the helical steel may contribute to the cracking torque value or different degrees of precracking and prestress losses are reducing the capacity of the specimens.

Torsional stiffness before cracking

The stiffness increased with the increase in pole diameter and wall thickness. The average stiffness for the 165 group experimental specimens was 1955 kN-m^2/rad (4730 kip-ft^2/rad). The control specimen P-1 (165-C), with visible longitudinal precracking, exhibited a reduced stiffness. Without specimen P-1, the average stiffness for the 165 group was 2068 kN-m^2/rad (5003 kip-ft^2/rad). The 210 group specimens had an average stiffness of 4483 kN-m^2/rad (10,846 kip-ft^2/rad).

Precracking torsional response of the poles was modeled using linear elastic torsional models (**Fig. 9**). Because

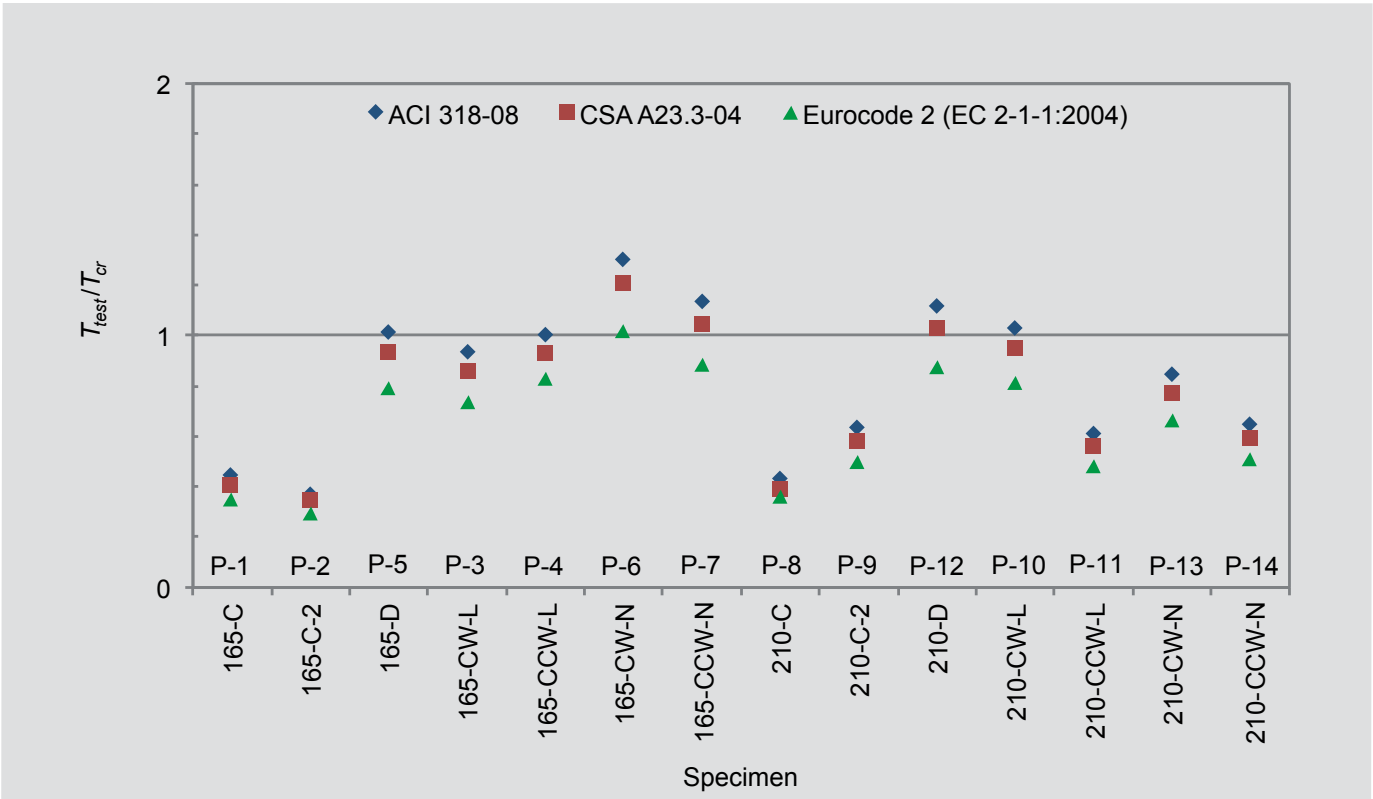

Figure 8. Comparison between code cracking torque predictions and test results. Note: T_{cr} = predicted cracking torque at 0.6 m (2 ft) from tip; T_{test} = cracking torque measured at 0.6 m from tip; ratio < 1.0 indicates unconservative code prediction.

all poles from the same group (165 or 210) had similar precracking stiffness, a comparison was made with the theoretical stiffness calculated using parameter values from Table 2 instead of individual specimen characteristics and values. Equations (7) and (8) are the elastic torsion formulas used for torsional stiffness.[20]

Table 5. Comparison of average values of T_{test}/T_{cr} using ACI-318-08, CSA A23.3-04, and Eurocode 2 statistical data with and without control specimens

		ACI 318-08		CSA A23.3-04		EC 2-1-1:2004	
		0.6 m from tip	Actual failure location	0.6 m from tip	Actual failure location	0.6 m from tip	Actual failure location
Average T_{test}/T_{cr} ratios with control specimens	Average	0.83	0.65	0.76	0.60	0.65	0.51
	Standard deviation	0.30	0.25	0.28	0.23	0.23	0.20
	High	1.31	1.10	1.21	1.02	1.02	0.86
	Low	0.37	0.35	0.34	0.32	0.29	0.28
	COV	0.36	0.39	0.36	0.39	0.36	0.39
Average T_{test}/T_{cr} ratios without control specimens	Average	0.97	0.76	0.89	0.70	0.76	0.60
	Standard deviation	0.22	0.22	0.20	0.21	0.17	0.18
	High	1.31	1.10	1.21	1.02	1.02	0.86
	Low	0.62	0.42	0.57	0.39	0.48	0.33
	COV	0.22	0.29	0.22	0.30	0.22	0.30

Note: COV = coefficient of variation; T_{cr} = theoretical cracking torque; T_{test} = experimental cracking torque. 1 m = 3.281 ft.

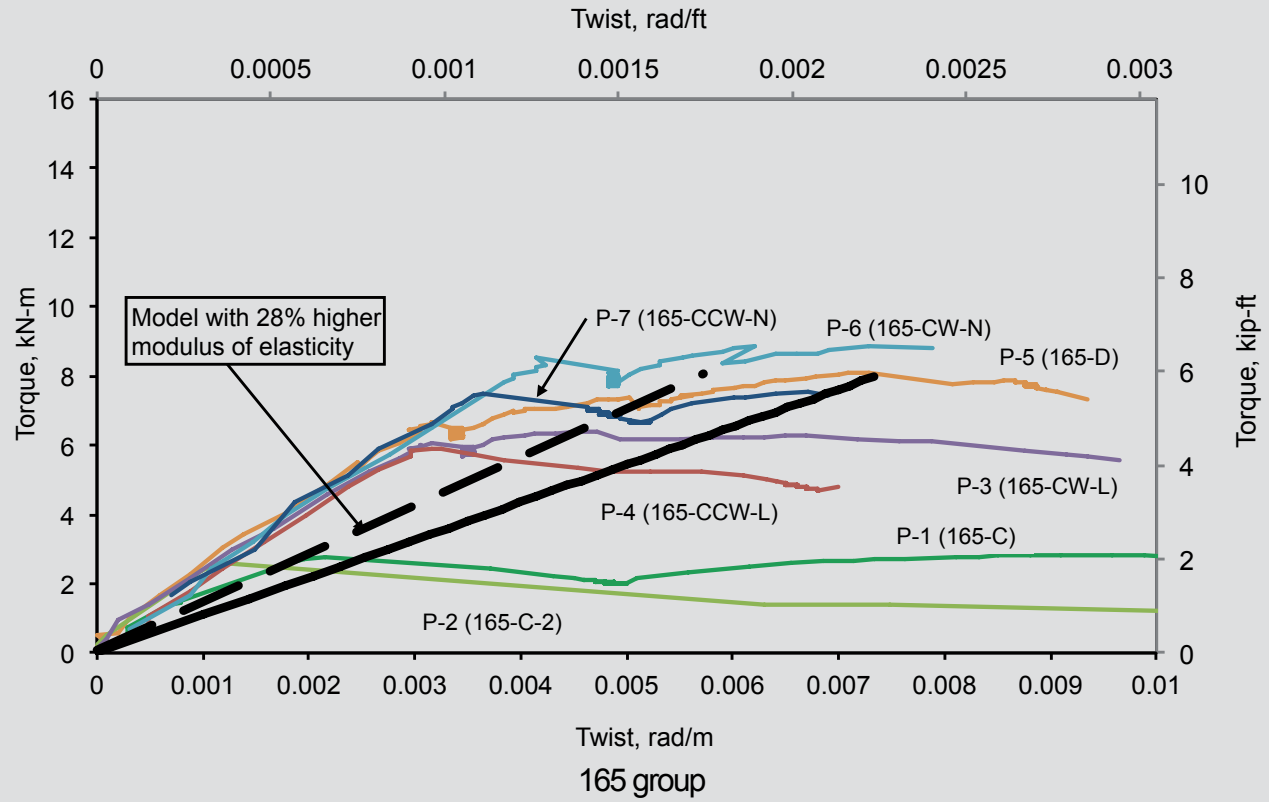

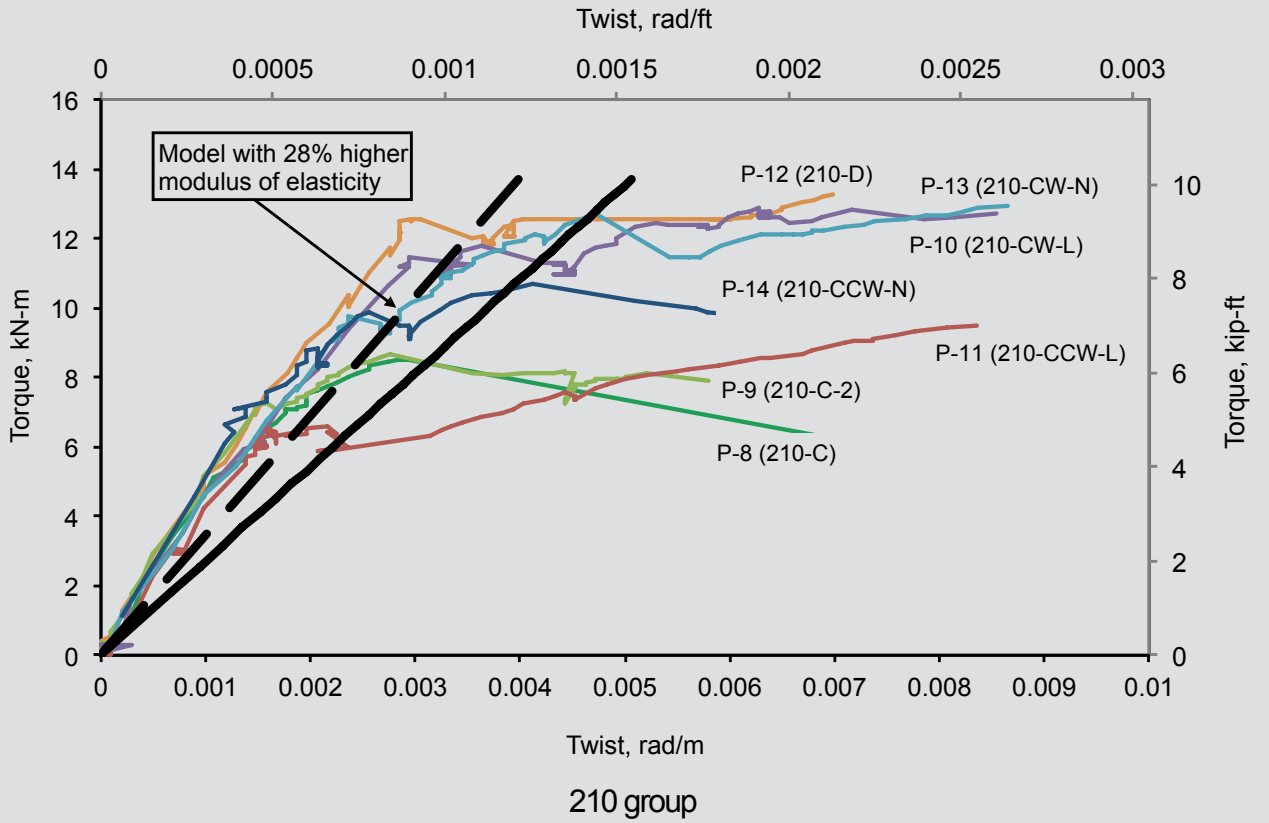

Figure 9. Linear elastic torsional predicted response compared with test results. Note: Average experimental stiffness 165 group = 2068 kN-m²/rad; average experimental stiffness 210 group = 4483 kN-m²/rad. 1 m = 3.281 ft; 1 kN = 0.225 kip.

$$T = \tau \frac{J}{c} \quad (7)$$

where

c = radius to point under analysis (T_{max} when $c = c_2$)

J = polar moment of inertia

$$= \frac{1}{2}\pi(c_2^4 - c_1^4)$$

c_2 = radius to the outside of the cross section

c_1 = radius of the inner hole of the pole

$$K_s = \frac{T}{\phi} = \frac{JG}{L} \quad (8)$$

where

K_s = torsional stiffness

ϕ = twist of the pole, in radians

L = test length of the pole

G = shear modulus of concrete

$= 0.3E_c$

E_c = modulus of elasticity of concrete

$= 5500\sqrt{f'_c}$ (in MPa)[21]

The biaxial stress added due to prestressing is included using the Mohr's circle prestressing factor $\sqrt{1 + \frac{f_{pc}}{f_t}}$.

The resulting formulas for torque and stiffness are Eq. (9) and (10).

$$T = \tau \frac{J}{c}\sqrt{1 + \frac{f_{pc}}{f_t}} \quad (9)$$

$$K_s = \frac{T}{\phi}\sqrt{1 + \frac{f_{pc}}{f_t}} = \frac{JG}{L}\sqrt{1 + \frac{f_{pc}}{f_t}} \quad (10)$$

The elastic stiffness calculated using Eq. (8) approximates the 210 group test stiffness well (Fig. 9). The theoretical stiffness is lower than that observed experimentally. The elastic formula does not approximate the 165 group results as well. According to Terrasi and Lees,[5] the difference between prediction and results can be attributed to the assumed shear modulus value and differences in wall thickness. Fouad et al.[2] suggest that spun-cast concrete poles can have a modulus of elasticity 28% higher than regular concrete. Increasing the assumed modulus of elasticity E_c by 28% to 48,845 MPa (7,085 ksi) from 42,603 MPa (6,179 ksi) brings the predictions closer to the test results for both the 165 and 210 group specimens. The predicted stiffness for the 165 and 210 groups using the 28% increased E_c value were 1392 kN-m^2/rad (3368 kip-ft^2/rad) and 3468 kN-m^2/rad (8390 kip-ft^2/rad), respectively. Modeling the specimens as solid cylinders increased the stiffness by 5% to 7%. The close prediction of stiffness by the linear elastic torsion formula indicates that the specimens were likely uncracked before the peak failure load (cracking load).

Postpeak load behavior

The compression field theory[22] was used to model the postcracking region of the specimen response (**Fig. 10**). The compression field theory, implemented into the computer model, allows modeling of the postcracking behavior of the poles: the postcracking torque, twist, and ultimate load. Postcracking torsion theories rely on the transverse reinforcement to carry the torsional loads; 3.5-mm-diameter (0.14 in.) (modulus of elasticity equal to 200 GPa [29 ksi]) helical steel reinforcing was used in the model. Yielding was assumed to occur at a strain of 0.002 and failure at 0.008. The predicted failure mode was due to yielding (500 MPa [72,500 psi]) and ultimate tensile failure (600 MPa [87,000 psi]) of the transverse reinforcement. Only the clockwise reinforced specimens (P-3, P-5, P-6, P-10, P-12, and P-13) were modeled because, theoretically, the counterclockwise specimens should behave similarly to the control specimens (without helical reinforcement). The clockwise direction of the spirals caused tension in the helical steel, making them effective in resisting load. The counterclockwise direction resulted in compressive principal stresses along the direction of the spirals, making them ineffective in resisting torsion. In the double-helix specimens (P-5 and P-12), only half of the helical steel is effective in resisting torsion; therefore, they should behave similarly to the clockwise specimens with widely spaced spirals (P-3 and P-10).

Figure 10 compares the experimental results of specimens P-6 (165-CW-N), P-3 (165-CW-L), and P-5 (165-D) with the torsion models. Specimen P-6 (165-CW-N), which failed at the butt clamp, follows the P-6 (165-CW-N CFT) model prediction closely. Specimen P-5 (165-D) failed suddenly at the loading collar and did not carry much load after cracking. Thus, its behavior differs from the model. Specimen P-3 (165-CW-L) also failed at the butt clamp, but unlike specimen P-6 does not show any postcracking strength (Fig. 10).

Specimen P-13 (210-CW-N) was the only one in the 210 group that failed at the collar with sudden loss of strength.

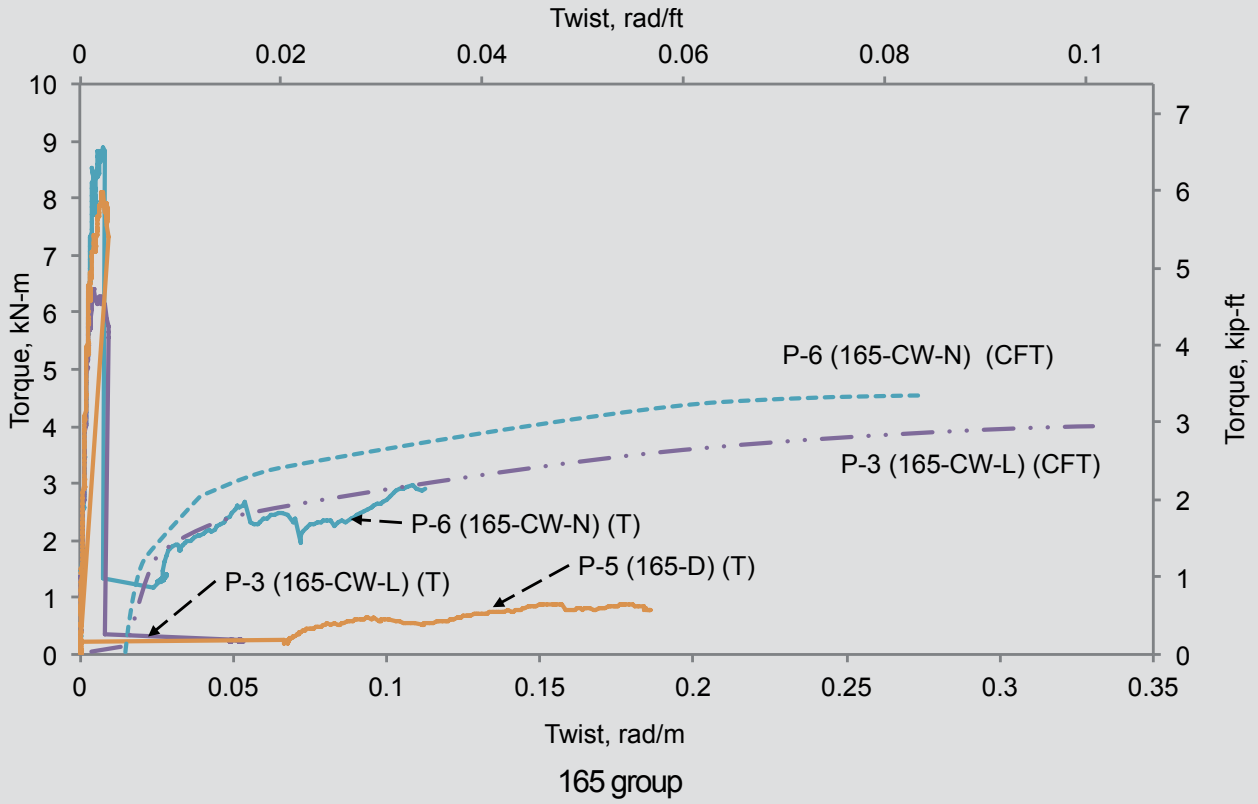

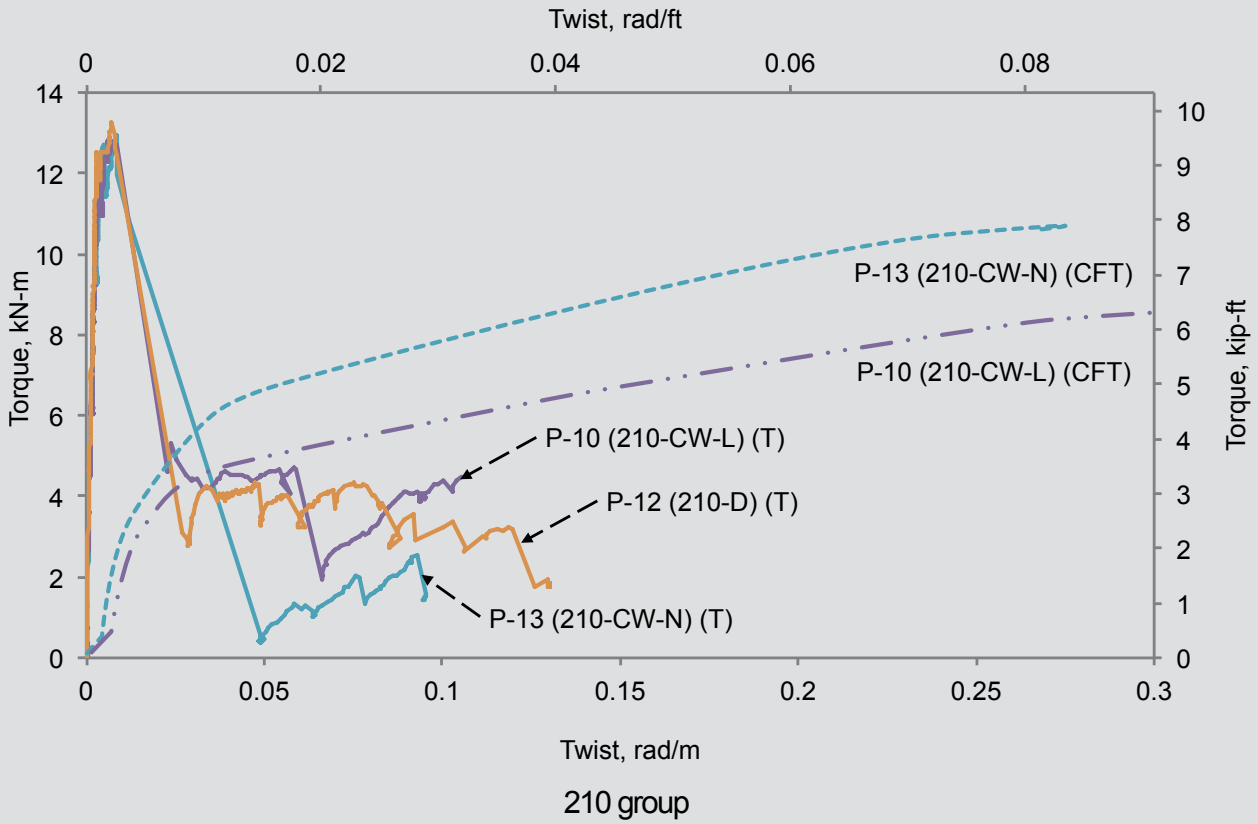

Figure 10. Torsional compression field theory theoretical postpeak response compared with test results. Note: CFT = theoretical (torsional compression field theory); T = torque-twist response of test specimen.

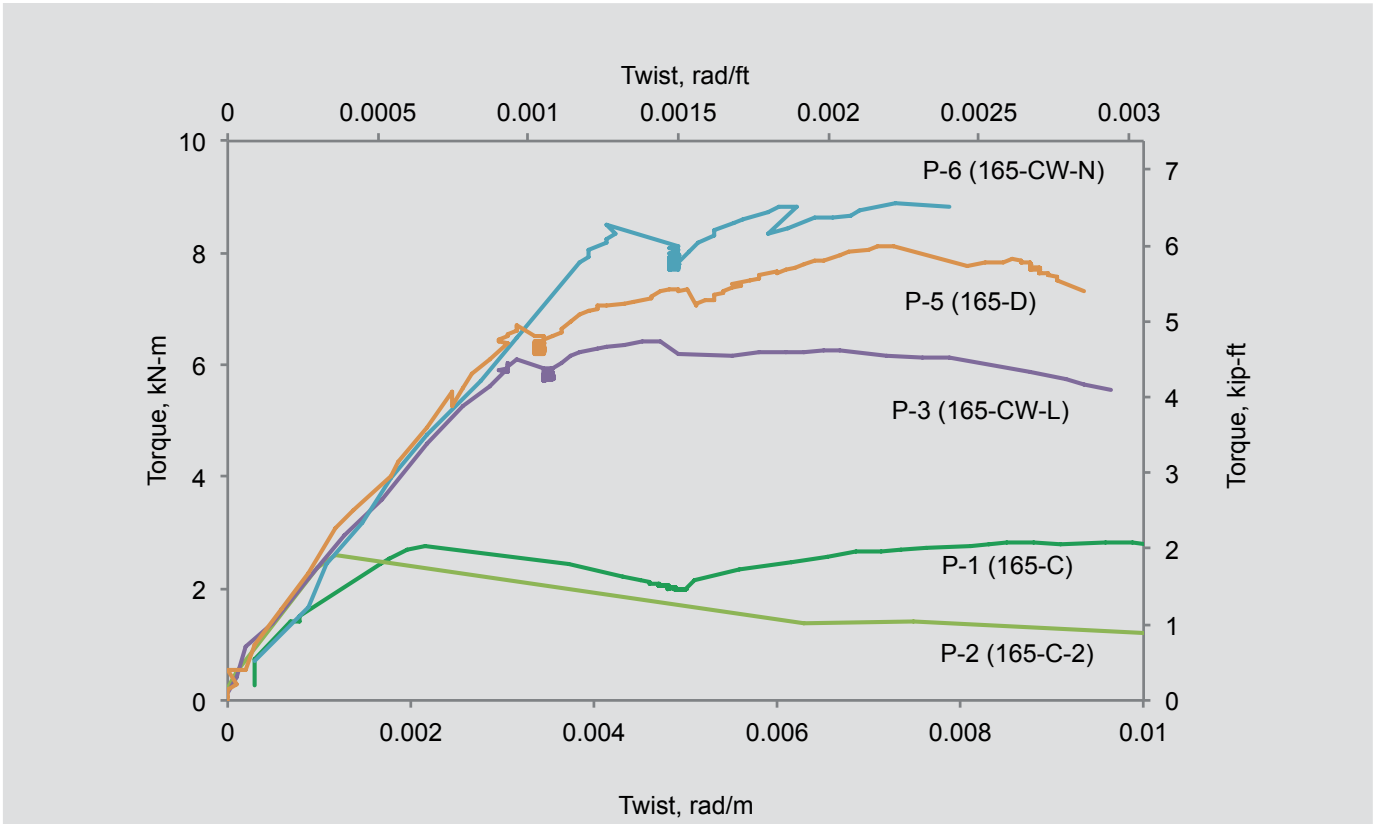

Figure 11. 165 mm tip diameter (165 group) clockwise and double-reinforced specimens. Note: 1 mm = 0.0394 in.

As a result, the predicted load history for specimen P-13 (210-CW-N) cannot be compared with the experimental results (Fig. 10). Specimens P-10 (210-CW-L) and P-12 (210-D) failed at the butt clamp and are compared with the model predictions for poles with widely spaced helical reinforcement. Specimen P-10 response follows the compression field theory model well to a twist of 0.06 rad/m. Specimen P-12 (210-D) follows the compression field theory model but fluctuates more. The close agreement between the model and the experimental results could indicate that the double helix specimen P-12 (210-D) actually behaved similarly to specimen P-10 (210-CW-L) as originally expected (that is, the other half helix of reinforcement is not active in load resistance).

Influence of helical reinforcing direction and spacing on cracking torque

Figures 11 through **14** show the plots of torque versus twist near the cracking zone. Both clockwise and counterclockwise reinforcing increased the torque capacity compared with the unreinforced control specimens of the 165 group. However, little difference was observed between the two methods of reinforcing (Fig. 11 and 12). The same can be said for the larger 210 group specimens (Fig. 13 and 14). Specimen P-13 (210-CW-N) cracked earlier than specimen P-10 (210-CW-L) but achieved the same ultimate torque. Specimen P-11 (210-CCW-L) cracked earlier than specimen P-14 (210-CCW-N) and also reached the same ultimate torque.

The cracking torque values for both the large- and normal-spacing specimens, regardless of the direction of the helix reinforcement, are close to each other. Therefore, for the 165 group, the direction of the helix reinforcement has little influence on torsional capacity (Fig. 11 and 12). Similarly, for the 210 group (excluding specimen P-11 [210-CCW-L], which seems to have cracked early due to errors in concrete batching and placement), it appears that direction of reinforcement has little influence on torsional capacity (Fig. 13 and 14).

The spacing of the helical reinforcement appears to have more effect on cracking torque than the direction of the reinforcement. The 165 group normal-spaced specimens (P-6 [165-CW-N] and P-7 [165-CCW-N]) had higher cracking torque values than the specimens with wider spacing (P-3 [165-CW-L] and P-4 [165-CCW-L]). Specimens P-6 (165-CW-N), P-7 (165-CCW-N), and P-5 (165-D), cracked at 8.5 kN-m, 7.5 kN-m, and 6.7 kN-m (6.3 kip-ft, 5.5 kip-ft, and 4.9 kip-ft), respectively. The cracking torque values for specimens P-3 (165-CW-L) and P-4 (165-CCW-L) were 6.1 kN-m and 5.9 kN-m (4.5 kip-ft and 4.4 kip-ft), respectively (Fig. 11 and 12). Cracking of the control specimens occurred at lower torque than all reinforced specimens.

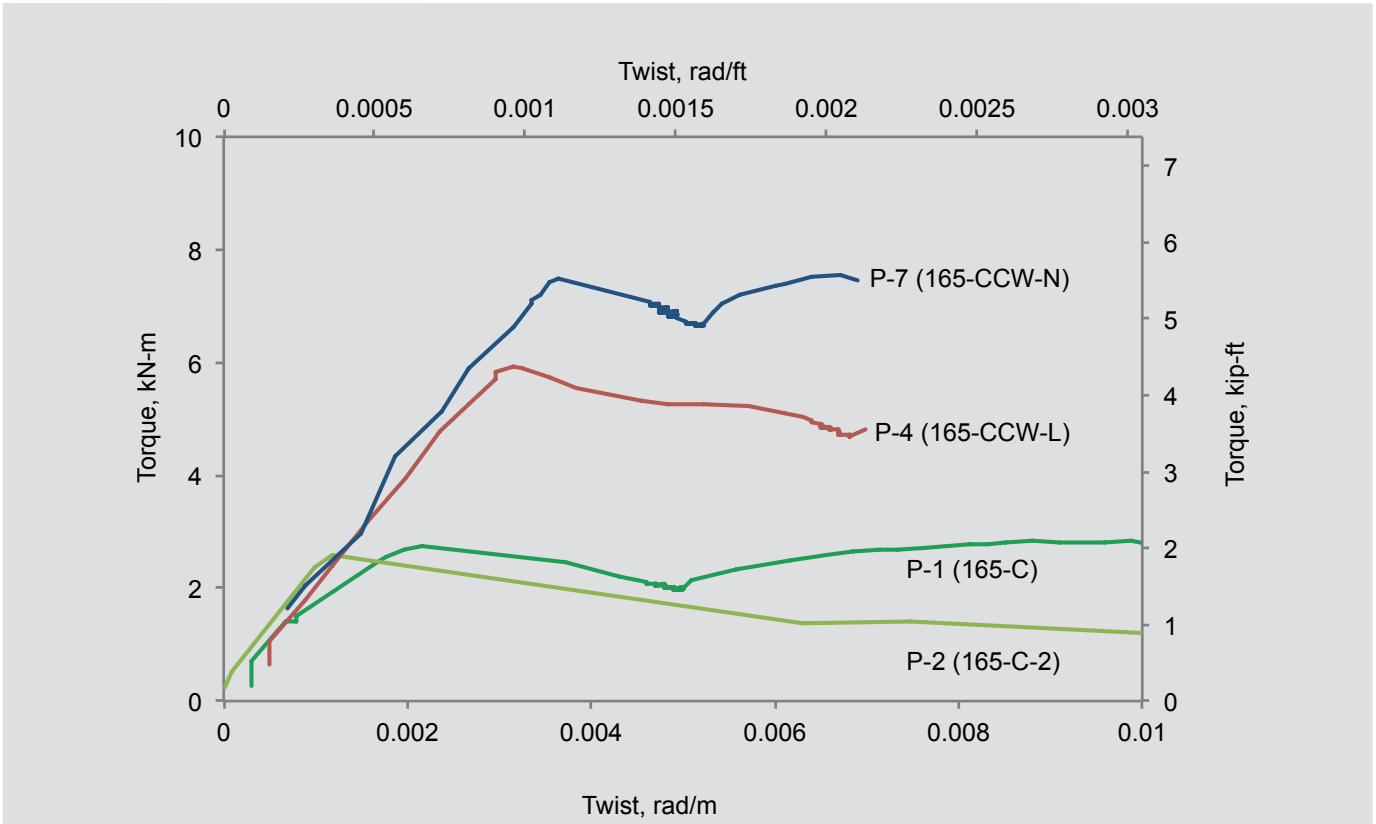

Figure 12. 165 mm tip diameter (165 group) counterclockwise reinforced specimens. Note: 1 mm = 0.0394 in.

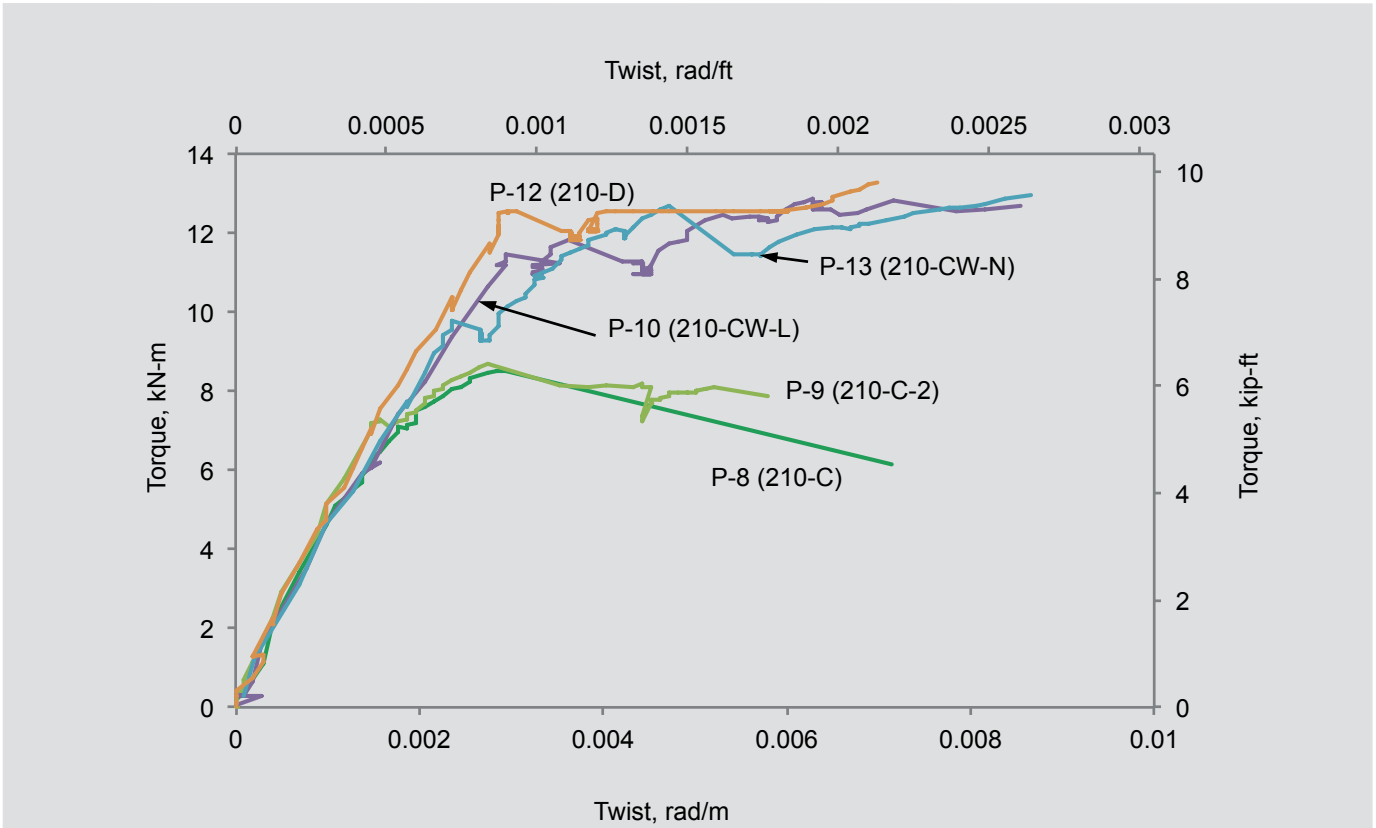

Figure 13. 210 mm tip diameter (210 group) clockwise and double-reinforced specimens. Note: 1 mm = 0.0394 in.

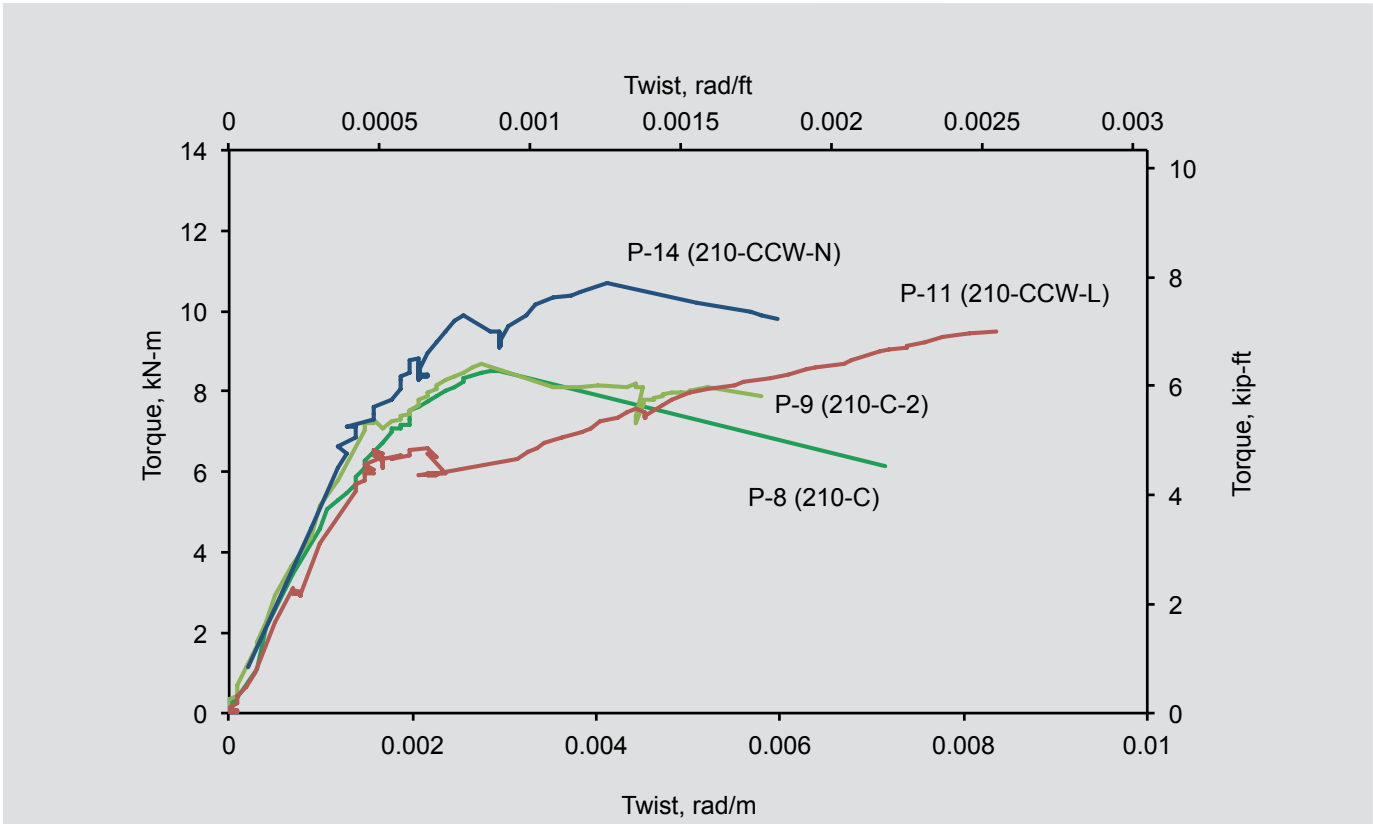

Figure 14. 210 mm tip diameter (210 group) counterclockwise reinforced specimens. Note: 1 mm = 0.0394 in.

The lower torsional capacities of the control specimens are likely due to longitudinal cracking observed along the prestressing strands. Without any helical reinforcing, the thin-walled 165 group poles were susceptible to cracking due to the transfer of the prestressing (more so than the 210 group poles, which had thicker walls).

The 210 group does not show a definite relationship between cracking load and spiral spacing as the 165 group did. The 210 group specimens had thicker walls and narrower spiral spacing (for both -N and -L specimens, P-10 to P-14) than the 165 group specimens (due to CSA A14-07 requirements). Specimens P-10 (210-CW-L) and P-13 (210-CW-N) cracked at 11.5 kN-m and 9.8 kN-m (8.5 kip-ft and 7.2 kip-ft), respectively, but later both continued to carry increasing load up to 12.9 kN-m (9.5 kip-ft). Specimen P-14 (210-CCW-N) cracked at 7.1 kN-m (5.2 kip-ft) but continued to carry increasing load up to 10.7 kN-m (7.9 kip-f). Specimen P-12 (210-D) cracked at 12.5 kN-m (9.2 kip-ft) and sustained load up to 13.3 kN-m (9.8 kip-ft). Specimen P-11 (210-CCW-L) appeared to have cracked at a lower load, possibly due to some error in manufacturing, but continued to carry increasing torsional load (Fig. 13 and 14). The control specimens P-8 (210-C) and P-9 (210-C-2) showed similar behavior to that of the counterclockwise specimens (Fig. 14); their cracking loads are slightly lower than counterclockwise specimens.

Conclusion

The experimental results and calculations using linear and nonlinear torsion models suggest that helical reinforcing steel in concrete poles is most important in preventing cracking of concrete during the release of prestressing strands. In all specimens tested in this research program, the maximum torsional capacities corresponded to the cracking torques. Postpeak behavior, even in heavily spiral-reinforced specimens, is brittle and results in rupture of the helical steel. Avoiding longitudinal precracking due to prestress prevents early torsion cracks originating from the longitudinal cracks. Cracking caused by improper transfer of the prestress force could cause additional loss of prestress in the pole, which has a negative effect on bending, shear, and torsional capacity. The helical steel may also affect cracking torque by confining the concrete core or by intercepting initial microcracking.

Concrete tensile strength is an important factor in the torsional strength of prestressed concrete poles. Therefore, improper concrete mixing or placement that causes segregation, cracking, and weaker zones of concrete due to inhomogeneity will all have a negative effect on concrete tensile strength and torsional cracking resistance.

Based on the test results and subsequent analysis, the following conclusions are offered:

- The torsional failure mode for concrete poles is brittle, with no postcracking ductility provided by the helical reinforcing steel.

- Helical reinforcing may influence the cracking torque capacity of the prestressed concrete pole; however, the primary function of the helical steel is for prestressing force transfer and minimizing longitudinal cracking.

- Spacing of the helical reinforcement is important because narrower spacing of helical reinforcement increased the torsional capacity, likely by limiting longitudinal cracking.

- The experimental cracking torque values were best predicted by ACI-318-08. The average code-predicted values for all codes were unconservative and with large scatter.

- For poles subject to high torsional loads, torsional reinforcement must be properly designed according to the codes of concrete practice. Relying on simplified rules for spacing of spiral reinforcement does not ensure high torsional strength and postpeak ductility.

Further testing of the minimum reinforcing values and transfer zone reinforcement for prestressed poles is required. From the current research, it may be possible to simplify the provisions of CSA A14-07 with regard to minimum reinforcing requirements and torsional capacities.

Acknowledgments

The authors want to express their gratitude for the support received by Sky Cast Inc. and the Natural Sciences and Engineering Council of Canada for the research undertaken. Thanks and gratitude are also expressed to the Ontario Graduate Scholarship program for the first author's scholarship to carry out the research.

References

1. Technical Committee on Concrete Poles. 2007. *Concrete Poles*. CSA A14-07. Mississauga, ON, Canada: Canadian Standards Association International.

2. Fouad, F. H., N. L. Scott, E. Calvert, and M. Donovan. 1994. Performance of Spun Prestressed Concrete Poles during Hurricane Andrew. *PCI Journal*, V. 39, No. 2 (March–April): pp. 102–110.

3. Chahrour, A. H., and K. A. Soudki. 2006. Structural Retrofitting of Deteriorated Concrete Lighting Poles Using FRP Sheets in Wet Layup—Field Application. *ASCE Journal of Composites for Construction*, V. 10, No. 3 (May–June): pp 234–243.

4. Rosson, B. T., J. R. Rohde, and R. Klovsky. 1996. Behavior and Design of Static Cast Prestressed Concrete Distribution Poles. *PCI Journal*, V. 41, No. 5 (September–October): pp. 94–107.

5. Terrasi, G. P., and J. M. Lees. 2003. CFRP Prestressed Concrete Lighting Columns. In *Field Applications of FRP Reinforcement: Case Studies*, SP 215, pp. 55–74. Farmington Hills, MI: American Concrete Institute (ACI).

6. Ghosh, R. S., and G. A. Senkiw. 1978. Load Testing of Prestressed Concrete Transmission Pole and Its Concrete Footing. *Canadian Journal of Civil Engineering*, V. 5 No. 2 (June): pp. 274–281.

7. Dilger, W. H., and A. Ghali. 1986. Response of Spun Cast Concrete Poles to Vehicle Impact. *PCI Journal*, V. 31, No. 1 (January–February): pp. 62–82.

8. Fouad, F. H., D. Sherman, and R. J. Werner. 1992. Spun Prestressed Concrete Poles—Past, Present, and Future. *Concrete International*, V. 14, No. 11 (November): pp. 25–29.

9. Subcommittee C27.20. 2006. *Standard Specification for Spun Cast Prestressed Concrete Poles*. ASTM C 1089-06. West Conshohocken, PA: ASTM International.

10. ASCE Task Force/PCI Committee on Concrete Poles and PCI Committee on Prestressed Concrete Poles. 1997. ASCE-PCI Committee Report: Guide for the Design of Prestressed Concrete Poles. *PCI Journal*, V. 42, No. 6 (November–December): pp. 93–134.

11. Technical Committee on Reinforced Concrete Design. 2004. *Design of Concrete Structures*. CSA A23.3-04. Mississauga, ON, Canada: Canadian Standards Association International.

12. ACI Committee 318. 2008. *Building Code Requirements for Structural Concrete (ACI 318-08) and Commentary (ACI 318R-08)*. Farmington Hills, MI: ACI.

13. Subcommittee B/525. 2004. *Eurocode 2: Design of Concrete Structures*, *Part 1-1: General Rules and Rules for Buildings*. BS EN 1992-1-1:2004: London, England: British Standards Institution.

14. Kuebler, M. 2008. *Torsion in Helically Reinforced Prestressed Concrete Poles*. Master's thesis. Waterloo, ON, Canada: University of Waterloo.

15. MagGregor, J. G., and M. G. Ghoneim. 1995. Design for Torsion. *ACI Journal*, V. 92, No. 2 (March–April): pp. 211–218.

16. Hsu, T. T. C. 1984. *Torsion of Reinforced Concrete*. New York, NY: Van Nostrand Reinhold Inc.

17. Highways Subcommittee on Bridges and Structures. 2009. *Standard Specification for Structural Supports for Highway Signs, Luminaries and Traffic Signals*. AASHTO LTS-5-M. Washington, DC: American Association of State Highway and Transportation Officials.

18. Technischen Komitee CEN/TC 229. 2004. *Betonfertigteile—Maste* [Precast Concrete Products—Masts and Poles]. DIN EN 12843:2004. Berlin, Germany: Deutsche Institut für Normung eV.

19. Technischen Komitee CEN/TC 50. 2006. *Lichtmaste—Teil 4: Anforderungen an Lichtmaste aus Stahl- und Spannbeton* [Lighting Columns—Part 4: Requirements for Reinforced and Prestressed Concrete Lighting Columns]. DIN EN 40-4:2005. Berlin, Germany: Deutsche Institut für Normung eV.

20. Beer, F. P., and E. R. Johnston. 1992. *Mechanics of Materials*. 2nd ed. SI units. New York, NY: McGraw Hill Book Co.

21. Collins, M. P., and D. Mitchell. 1987. *Prestressed Concrete Basics*. Ottawa, ON, Canada: Canadian Prestressed Concrete Institute.

22. Mitchell, D., and M. P. Collins. 1974. Diagonal Compression Field Theory: A Rational Model for Structural Concrete in Pure Torsion. *ACI Journal*, V. 71, No. 8 (August): pp. 396–408.

Notation

A = total area of the cross section including hollow areas

A_{cp} = area enclosed by perimeter p_{cp}

A_k = area enclosed by centerline of shear flow, including hollow area

A_o = area enclosed by shear flow path

A_s = area of one helix

c = radius to point under analysis

c_1 = radius of inner hole

c_2 = radius to outside of cross section

E_c = modulus of elasticity of concrete

f_c' = concrete compressive strength

f_{ck} = characteristic concrete compressive strength (European equivalent to f_c')

f_{cm} = mean compressive strength at 28 days

f_{ctd} = design concrete tensile strength

f_{ctm} = mean axial tensile strength

f_{pc} = stress in concrete section due to prestressing

f_t = concrete tensile strength

G = shear modulus of concrete

J = polar moment of inertia

K_s = torsional stiffness

L = test length of pole

p_{cp} = perimeter of concrete section

s = spacing of helical reinforcement

t = thickness of member

$t_{ef,i}$ = effective wall thickness

T = applied torque

T_{cr} = theoretical cracking torque

T_{test} = experimental cracking torque

u = circumference of cross section

w = wall thickness

ρ_s = reinforcement percentage

τ = shear stress due to torsion

ϕ = twist of pole, in radians

About the authors

Michael Kuebler, MASc, EIT, is a designer at Formation Engineering in Vaughan, ON, Canada. He received his MASc from the University of Waterloo in Waterloo, ON, Canada.

Maria Anna Polak, PhD, P.Eng, is a professor in the Department of Civil and Environmental Engineering at the University of Waterloo.

Abstract

This paper focuses on the effect of the transverse reinforcement—its amount, spacing, and direction—on torsional strength in an effort to simplify the governing codes and provide general information on the behavior of spun-cast prestressed concrete poles under pure torsion. The rationale behind the typical code values for spacing and direction of the transverse reinforcement is not apparent. A total of 14 specimens were produced as part of a testing program. The testing program consisted of two groups of seven specimens with two different tip diameters: 6.5 in. (165 mm) and 8.3 in. (210 mm). Within each group the spacing and direction of the wound helical transverse reinforcement was varied. Each specimen was clamped at the butt end, and a counterclockwise torque load was applied at 2 ft (0.6 m) from the tip end. Applied torque and rotation of the tip were recorded using an inline load cell and electronic clinometers. The test concluded when the rotation reached approximately 13° to 15° or failure occurred. Experimental cracking torque values were compared with code-calculated theoretical values using current codes. Precracking and postcracking torque-twist responses were analyzed with elastic torsion and torsional compression field theory models. It was concluded that the primary function of the transverse reinforcement is to minimize the longitudinal precracking due to prestressing transfer forces. The prestressed concrete pole failure mode in torsion is brittle and sudden, and the transverse reinforcement provides no postcracking ductility.

Keywords

Cracking, pole, reinforcement, spin casting, torque, torsion.

Review policy

This paper was reviewed in accordance with the Precast/Prestressed Concrete Institute's peer-review process.

Reader comments

Please address any reader comments to journal@pci.org or Precast/Prestressed Concrete Institute, c/o *PCI Journal* 200 W. Adams St., Suite 2100, Chicago, IL 60606.